空间电动绳系推进中导电系绳动态特性分析

李 然, 许 滨, 张 珩
(中国科学院 力学研究所技术发展部,北京 100080)

摘 要: 通过建立空间电动绳系系统动力学模型,研究了通有电流的导电系绳高速运动切割地球磁力线时系绳的振荡和变形特性。通过数值计算,分别给出了导电系绳在不同长度和不同主子星质量比下对系绳动态特性的影响,得到了一些规律性认识和结果。

关键词: 空间电动绳系;系绳;振荡;频率
中图分类号: V11; V412.4+1 **文献标识码**: A

空间电动绳系推进是一种无需燃料的航天器轨道机动技术。其基本原理是在导电系绳两端分别安装等离子收集器和发射器,一端从外界电离层中收集电子,另一端向外界发射电子,从而构成开放的电流回路。通有电流的系绳高速运动切割地磁线,与地球磁场相互作用而产生作用于系绳上的连续推力,从而实现航天器的轨道机动[1,2]。

细长(几千米~几十千米)导电系绳在高速运动过程中的振荡和变形影响航天器姿态,从而导致航天器无法完成预定目标任务。Iess描述了利用电动绳系技术降低卫星轨道原理并进行简单分析[3]。Corsi对导电系绳展开/回收过程中系绳稳定性进行了分析与研究,给出了一些速率、张力等控制方法[4]。Emmanuel Vienet将空间导电绳系系统简化为单摆模型进行轨道平面内运动分析,给出通过电流控制系绳振动[5]。鉴此,本文以系绳空间三个位置坐标和系绳张力等4个参数作为参变量,建立空间电动绳系推进过程中轨道飞行动力学模型,并在此基础上,通过数值计算,分析了导电系绳在轨道运动过程中的动态特性。

1 导电系绳轨道飞行动力学建模

1.1 模型简化

结合研究问题的特殊性对空间电动绳系系统和外部空间环境做了如下假设:

1) 将子母航天器(主子星)简化为质点,不考虑其体积和姿态;

2) 导电系绳看作均匀柔软系绳,质量沿绳长均匀分布,无弹性伸长;

3) 系统的运动中心和质心重合,初始状态,绳系绷紧伸直,方向指向地心;

4) 只考虑地球引力和安培力的影响;

5) 不考虑地球偏转率的影响,且引力常数为定值;

6) 电磁场采用偏心倾斜双极子模型;

7) 假定绳系所在空间电子浓度足够大,等离子收发器收发电流的能力足够强,不对系统中的电流产生附加约束。

1.2 坐标系的建立

在建模过程中,首先建立了以下3个坐标系,即地心赤道惯性坐标系 $OXYZ$、标准地磁场坐标系 $O_1X_1Y_1Z_1$ 和轨道坐标系 $O_2X_2Y_2Z_2$ 如图1所示。惯性坐标系的原点在地心,X 轴在赤道面上并指向春分点,Z 轴指向地理北极,Y 轴方向由右手系决定;地磁坐标系以需要计算地磁场的点为原点,其 X_1 轴沿水平面指向正北方向,Z_1 轴指向地心,Y_1 轴方向由右手系决定;轨道坐标系的原点在绳系的质心,X_2 轴指向轨道飞行方向,Z_2 轴指向地心,Y_2 轴方向由右手系决定。在研究系绳的变形时,建立了系绳微元 ΔL 惯性主轴系 $O_iX_4Y_4Z_4$ 如图2,Z_4 轴与系绳微元重合,X_4 轴

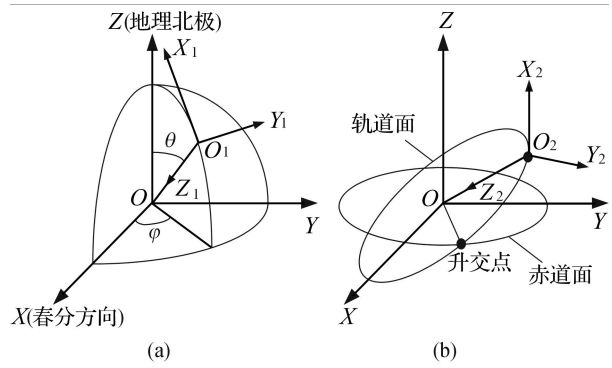

图 1 惯性坐标系、地磁坐标系与轨道坐标系

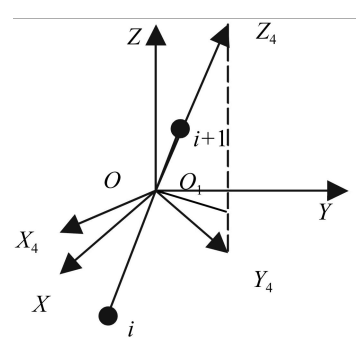

图 2 系绳微元 ΔL 惯性主轴系

基金项目: 总装预研基金(9140A200603062K0401)
收稿日期: 2007-08-21 修改稿收到日期: 2007-09-29
第一作者 李 然 女,硕士生,1981年生

© 1994-2009 China Academic Journal Electronic Publishing House. All rights reserved. http://www.cnki.net

固定在 XOY平面上, Y_4 轴由右手系决定。

1.3 运动方程的建立

由于柔性系绳的弯曲变形,不能建立整个绳系的运动方程,所以将系绳等分为 n段,它们之间通过无摩擦的万向旋转头连接,在满足位移连续条件和力的平衡条件下,建立每个微元的运动方程。设每段长为 ΔL, 质量为 Δm,当 n取值足够大时,每段系绳可近似等效为均匀细杆。

根据牛顿第二运动定律得第 i段系绳微元 ΔL_i 的轨道运动方程为:

$$\begin{cases} \Delta m \ddot{x}_{o_i} = G_{x_i} + F_{x_i} - T_{x_i} + T_{x_{i+1}} \\ \Delta m \ddot{y}_{o_i} = G_{y_i} + F_{y_i} - T_{y_i} + T_{y_{i+1}} \\ \Delta m \ddot{z}_{o_i} = G_{z_i} + F_{z_i} - T_{z_i} + T_{z_{i+1}} \end{cases} \tag{1}$$

其中 $G_{x_i}, G_{y_i}, G_{z_i}$分别为系绳微元所受的地球引力在惯性坐标系三轴方向上的投影值, $F_{x_i}, F_{y_i}, F_{z_i}$分别为系绳微元所受的电磁力在惯性坐标系三轴方向上的投影值, $T_{x_i}, T_{y_i}, T_{z_i}$和 $T_{x_{i+1}}, T_{y_{i+1}}, T_{z_{i+1}}$分别为系绳微元两端的结点张力在惯性坐标系三轴方向上的投影值, $(x_{o_i}, y_{o_i}, z_{o_i})$是系绳微元中点位置坐标在地心惯性坐标系下的值, (x_i, y_i, z_i) $(i=1, 2\cdots\cdots n+1)$是系绳节点位置坐标在地心惯性坐标系下的值。

为了方便起见,将第 i段系绳中心 O_i 的加速度用第 i段系绳两端加速度均值来表示,得:

$$\begin{cases} \ddot{x}_i + \ddot{x}_{i+1} = 2(F_{x_i} + G_{x_i} - T_{x_i} + T_{x_{i+1}})/\Delta m \\ \ddot{y}_i + \ddot{y}_{i+1} = 2(F_{y_i} + G_{y_i} - T_{y_i} + T_{y_{i+1}})/\Delta m \\ \ddot{z}_i + \ddot{z}_{i+1} = 2(F_{z_i} + G_{z_i} - T_{z_i} + T_{z_{i+1}})/\Delta m \end{cases} \tag{2}$$

由牛顿第二运动定律得系绳两端点运动的边界条件:

$$\begin{cases} m_2 \ddot{x}_1 = T_{x_1} - \mu x_1 m_2 / r_1^3 \\ m_2 \ddot{y}_1 = T_{y_1} - \mu y_1 m_2 / r_1^3 \\ m_2 \ddot{z}_1 = T_{z_1} - \mu z_1 m_2 / r_1^3 \end{cases}$$

$$\begin{cases} m_1 \ddot{x}_{n+1} = - T_{x_{n+1}} - \mu x_{n+1} m_1 / r_{n+1}^3 \\ m_1 \ddot{y}_{n+1} = - T_{y_{n+1}} - \mu y_{n+1} m_1 / r_{n+1}^3 \\ m_1 \ddot{z}_{n+1} = - T_{z_{n+1}} - \mu z_{n+1} m_1 / r_{n+1}^3 \end{cases} \tag{3}$$

其中 m_1是主航天器总质量, m_2 为系绳下端悬挂的质量, r_i $(i=1, 2)$为两端点地心距, μ是地球引力常数。

由欧拉公式得系绳微元 ΔL_i 绕质心 O_i 的转动方程[6]:

$$\begin{cases} I_{x_{4i}} \dot{\omega}_{x_{4i}} + (I_{z_{4i}} - I_{y_{4i}}) \omega_{y_{4i}} \omega_{z_{4i}} = M_{x_{4i}} \\ I_{y_{4i}} \dot{\omega}_{y_{4i}} + (I_{x_{4i}} - I_{z_{4i}}) \omega_{z_{4i}} \omega_{x_{4i}} = M_{y_{4i}} \\ I_{z_{4i}} \dot{\omega}_{z_{4i}} + (I_{y_{4i}} - I_{x_{4i}}) \omega_{x_{4i}} \omega_{y_{4i}} = M_{z_{4i}} \end{cases} \tag{4}$$

其中 $\omega_{x_{4i}}$、$\omega_{y_{4i}}$和 $\omega_{z_{4i}}$为系绳 ΔL 绝对角速度 $\vec{\omega}$在惯性主轴系 $O_i X_4 Y_4 Z_4$ 中的分量, $M_{x_{4i}}$、$M_{y_{4i}}$和 $M_{z_{4i}}$为系绳微元 ΔL_i所受力矩 (对 O_i点的引力梯度力矩和张力矩)在惯性主轴系 $O_i X_4 Y_4 Z_4$ 中的分量, $I_{x_{4i}} = \frac{1}{12}\rho_l \Delta L^3$, $I_{y_{4i}} = \frac{1}{12}\rho_l \Delta L^3$, $I_{z_{4i}} = 0$, ρ_l为系绳线密度。

1) 系绳的空间表示

假设第 i段系绳微元与惯性坐标系 Z轴的夹角为 θ_{Li},其在 XOY平面上的投影点与 X 轴的夹角为 φ_{Li},则第 i段系绳的三个方向余弦为:

$$\begin{cases} \cos\alpha_{Li} = \sin\theta_{Li}\cos\varphi_{Li} \\ \cos\beta_{Li} = \sin\theta_{Li}\cos\varphi_{Li} \\ \cos\gamma_{Li} = \cos\theta_{Li} \end{cases} \tag{5}$$

则第 i段系绳 $D_i D_{i+1}$长度矢量是:

$$\Delta\vec{L}_i = \Delta L_i \cos\alpha_{Li}\vec{i} + \Delta L_i \cos\beta_{Li}\vec{j} + \Delta L_i \cos\gamma_{Li}\vec{k} \tag{6}$$

2) 感应电动势的计算

第 i段系绳微元 ΔL_i 高速运动切割地磁场磁力线产生的感生电动势 $\Delta\varepsilon_i$为:

$$\Delta\varepsilon_i = \Delta L_i \cdot (\vec{v}_{oi} \times \vec{B}_{oi}) \tag{7}$$

其中下标"O_i 表示第 i段系绳中点。其中 $\vec{v}_{oi}$是微元段系绳 ΔL_i 相对地球磁场的运动速度,即:

$$\begin{cases} v_{oix} = \dot{x}_t + \omega_e y_{oi} \\ v_{oiy} = \dot{y}_t + \omega_e x_{oi} \\ v_{oiz} = \dot{z}_t \end{cases} \tag{8}$$

上式中 $\dot{x}_t$、$\dot{y}_t$和 $\dot{z}_t$为系绳微元 ΔL_i 中点 O_i 在地球地心惯性坐标系下三个速度分量, ω_e 地球自转平均角速度。因 $\Delta L \ll r$,假设系绳微元段 ΔL_i 所在空间位置的地磁场强度相同,即第 i段系绳 ΔL_i 中点的地磁场强度 $\vec{B}_{oi}$。

3) 电磁力的计算

第 i段导电系绳 ΔL_i 切割地磁场所受到的电磁力为:

$$\vec{F}_i = I \cdot \Delta\vec{L}_i \times \vec{B}_{oi} \tag{9}$$

其中:

$$I = \frac{\sqrt{(P - 2P_c)(R_l + 2R_c) + \frac{\varepsilon^2}{4}} - \frac{\varepsilon}{2}}{R_l + 2R_c} \tag{10}$$

其中, R_l为导电系绳的电阻, R_c为电子收集/发射器的等效电阻(外界等离子体的电阻较小,这里予以忽略), ε为感应电动势, P为外加电源功率, P_c为每个电子收集/发射器的电源功耗。

2 算例与分析

2.1 数值计算

根据上面的运动方程经过进一步推导可以得到如下的数值计算公式:

© 1994-2009 China Academic Journal Electronic Publishing House. All rights reserved.　http://www.cnki.net

$$\begin{pmatrix} \ddot{x}_{i+1} \\ \ddot{y}_{i+1} \\ \ddot{z}_{i+1} \end{pmatrix} = T_{aai} \begin{pmatrix} \ddot{x}_i \\ \ddot{y}_i \\ \ddot{z}_i \end{pmatrix} + T_{tti} \begin{pmatrix} T_{x_i} \\ T_{y_i} \\ T_{z_i} \end{pmatrix} + H_{ai}$$

$$\begin{pmatrix} T_{x_{i+1}} \\ T_{y_{i+1}} \\ T_{z_{i+1}} \end{pmatrix} = T_{tai} \begin{pmatrix} \ddot{x}_i \\ \ddot{y}_i \\ \ddot{z}_i \end{pmatrix} + T_{tti} \begin{pmatrix} T_{x_i} \\ T_{y_i} \\ T_{z_i} \end{pmatrix} + H_{ti} \qquad (11)$$

其中 T_{aai}、T_{ati}、T_{tai}、T_{tti}、H_{ai}、H_{ti}均为 3 ×3的矩阵,这里略去不列。

设 $\begin{pmatrix} \ddot{x}_i \\ \ddot{y}_i \\ \ddot{z}_i \end{pmatrix} + T_{Mi} \begin{pmatrix} T_{x_1} \\ T_{y_1} \\ T_{z_1} \end{pmatrix} + H_{Mi}$ 和 $\begin{pmatrix} T_{x_i} \\ T_{y_i} \\ T_{z_i} \end{pmatrix} = T_{Ni} \begin{pmatrix} T_{x_1} \\ T_{y_1} \\ T_{z_1} \end{pmatrix} + H_{Ni}$

代入 (11)可以得到迭代计算矩阵和初始计算条件。将加速度值两次积分得到各节点位置坐标在地心惯性坐标系下的值 (x_i, y_i, z_i) $(i = 1, 2, \cdots\cdots n+1)$,通过坐标变换得到轨道坐标系下的位置坐标值 (x_{2i}, y_{2i}, z_{2i}) $(i = 1, 2, \cdots\cdots n+1)$。

为了进一步分析系绳的振荡,更加明确地看到系绳的变形情况,我们在轨道坐标系下对摆角做了如下定义:

轨道面内摆角: $\theta_{in} = \mathrm{arctg}\left(\dfrac{x_{2i+1} - x_{2i}}{z_{2i+1} - z_{2i}}\right)$

轨道面外摆角: $\theta_{out} = \mathrm{arctg}\left(\dfrac{y_{2i+1} - y_{2i}}{z_{2i+1} - z_{2i}}\right)$

其中 $(i = 1, 2\cdots\cdots n)$。

空间电动绳系飞行任务设计参数如表 1和表 2所示。其中, r为轨道的长半轴 (圆轨道时表示半径, km),λ为地球惯性坐标系中 X轴正方向的东经度,Ω为轨道面的升交点赤经, i为轨道倾角,τ为系统第一次通过升交点的时间, R_c为电子发射器的等效电阻 (Ω), R_A表示电子收集器的等效电阻 (Ω), ρ_R为导电系绳 (铝)的电阻率 (Ωm), ρ_m导电系绳 (铝)的密度 (kg/m^3), P_i为外电源功率 (W), m_1为主星质量 (kg), m_2为子星质量 (kg), m_l为导电系绳质量 (kg)。下标为 0的参数表示 $t = 0$时的初始值。

表 1 飞行任务基本参数

r_0	λ_0	Ω_0	i_0	τ
7 071	0 °	0 °	45 °	0

表 2 电动绳系系统参数

m_1	m_2	m_l	P_i
800	100	100	410
R_C	R_A	ρ_R	ρ_m
50	50	2. 826 ×10^{-8}	2 700

2 2 结果分析

根据上述条件,我们得到了数值计算结果和相应的曲线。

图 3给出了导电系绳在轨道坐标系上的投影曲线,其中 (a)为导电系绳在轨道平面内 $(O_2 X_2 Z_2)$的投影, (b)为导电系绳在轨道平面外 $(O_2 Y_2 Z_2)$的投影, t_1、t_2和 t_3分别对应系绳运动过程中的先后三个时间点,最小时间间隔为 $T/50$ (T = 5 914. 42 s)。

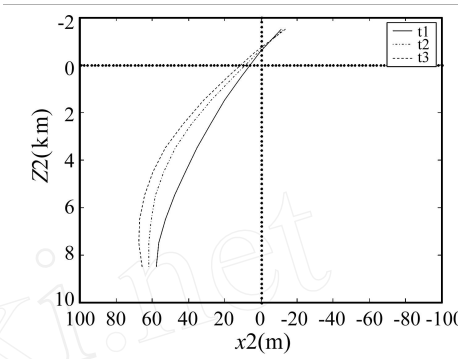

面内弯曲变形(系绳长度:10km)

(a)

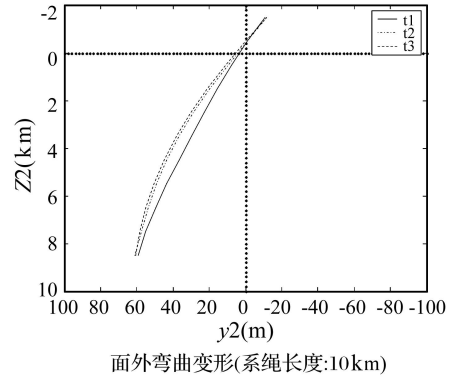

面外弯曲变形(系绳长度:10km)

(b)

图 3 系绳变形曲线

图 3可以看出在运动过程中,系绳产生横向振荡即基频摆动和高频振动两部分。频率最低的振荡称为摆动,其它所有频率较高的振荡统称为振动。

图 4分别给出了系绳运动过程中轨道面内和面外摆角的时域图和频谱图。时域图中可以看出长度 10km的系绳在运动过程中轨道面内最大摆角 θ_{in}在 - 0. 5 °~1. 3 °之间,轨道面外最大摆角 θ_{out}在 - 4 °- 5 之间。从摆角频谱图中我们找到了系绳运动过程中轨道面内外的主要震荡频率如表 3。从表 3中可以看出其轨道面内震荡角频率主要包含 ω_0, $\sqrt{3}\omega_0$, $3\omega_0$ (ω_0 = 1. 061 8 ×10^{-3} rad/s,是轨道运动的角频率)等频率成分;轨道面外振荡角频率主要包含 ω_0, $2\omega_0$, $6\omega_0$等频率成分。

表 3 10 km导电系绳震荡频率表

轨道面内频率		轨道面外频率	
ω_1	1. 062 4 ×10^{-3}	ω_1	1. 062 4 ×10^{-3}
ω_2	1. 832 6 ×10^{-3}	ω_2	2 124 7 ×10^{-3}
ω_3	3 186 8 ×10^{-3}	ω_3	6. 362 2 ×10^{-3}

图 5给出空间电动绳系系统轨道运行 66 h导电系绳振荡和变形特性。从中可看出对于同一系统,系绳轨道面内摆角要比面外摆角小,面内摆动的频率也比面外的小。

© 1994-2009 China Academic Journal Electronic Publishing House. All rights reserved. http://www.cnki.net

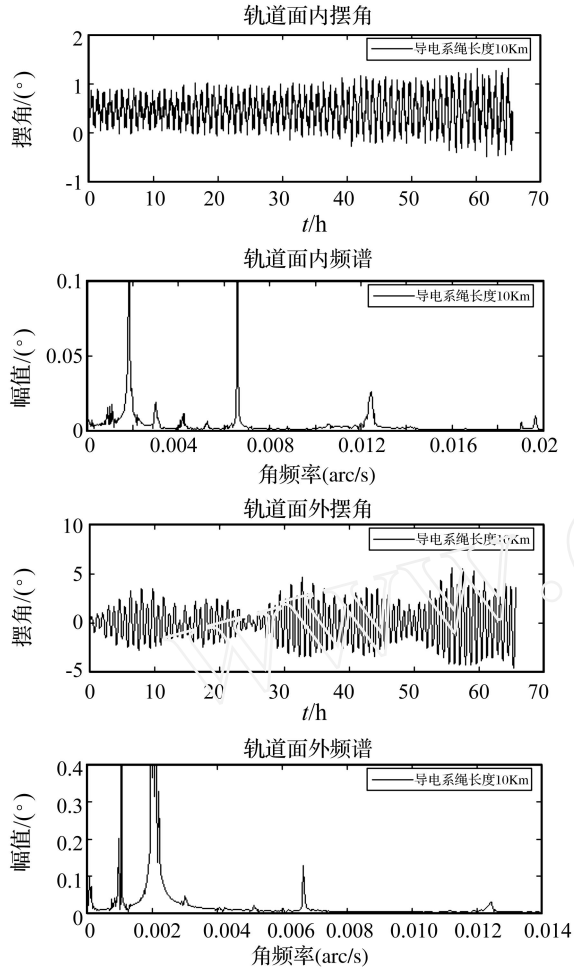

图 4　导电系绳摆角及振荡角频谱

图 6给出 5 km、10 km和 20 km等三种长度的导电系绳的振荡特性对比分析。从中可知长度的变化主要影响轨道面内振荡频率,对轨道面外而言仅影响其振动频率即高阶震荡频率。

图 7和图 8分别给出了主子星在不同质量比的条件下,系绳运动过程中轨道面内和面外摆角的频谱图和时域图。图中可以看出,主子星质量比越小,其导电系绳振荡频率成分越多,系绳振荡剧烈,严重影响导电系绳使用寿命。主子星质量比越小,随着电动绳系系统推进时间的增加,系统偏离铅垂线 (地心与绳系系统质心连线)角度逐渐增大,直至某一最大角度,此后保持该角度周期性地摆动。

3　结　束　语

通过所建立的空间电动绳系系统动力学模型,分析研究了导电系绳在高速运动过程中振荡和变形特性,获得了以下几点规律性认识:

1) 导电系绳轨道面内振荡角频率主要包含 ω_0, $\sqrt{3}\omega_0$, $3\omega_0$ 等成分,而轨道面外振荡角频率主要包含 ω_0, $2\omega_0$, $6\omega_0$ 等成分。

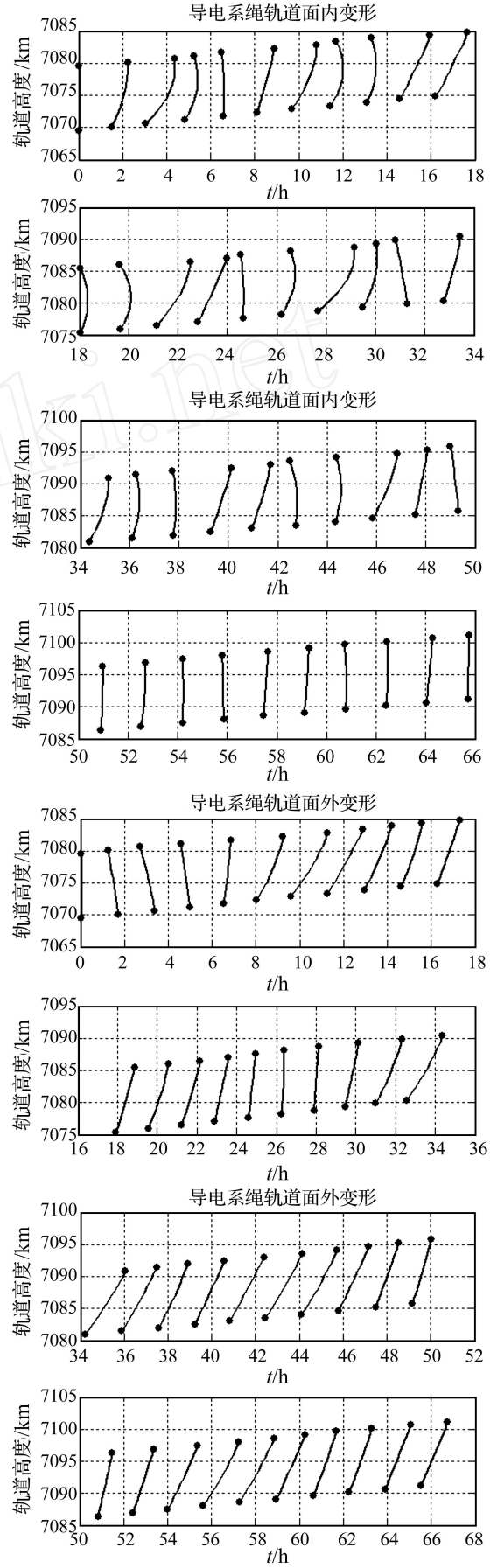

图 5　系绳随轨道高度变化变形示意图

© 1994-2009 China Academic Journal Electronic Publishing House. All rights reserved.　http://www.cnki.net

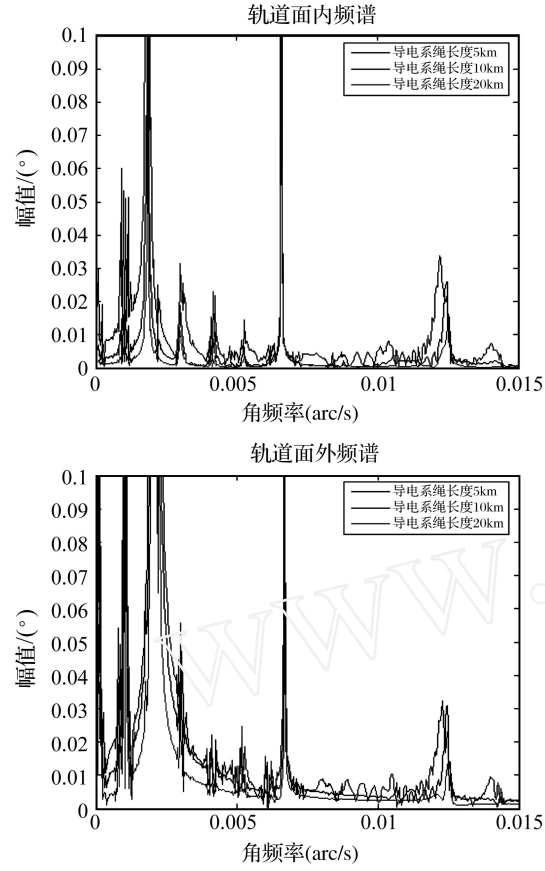

图 6 不同长度导电系绳振荡角频率谱

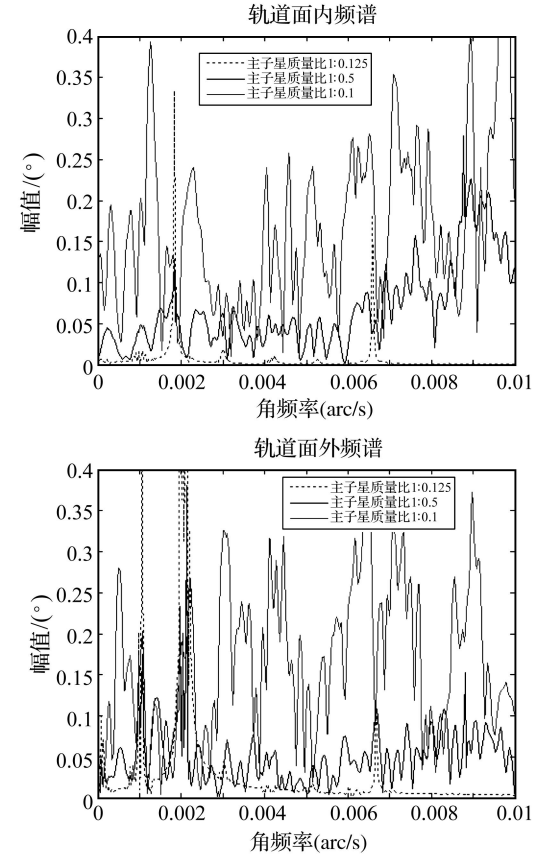

图 7 不同主子星质量比的导电系绳振荡角频率谱

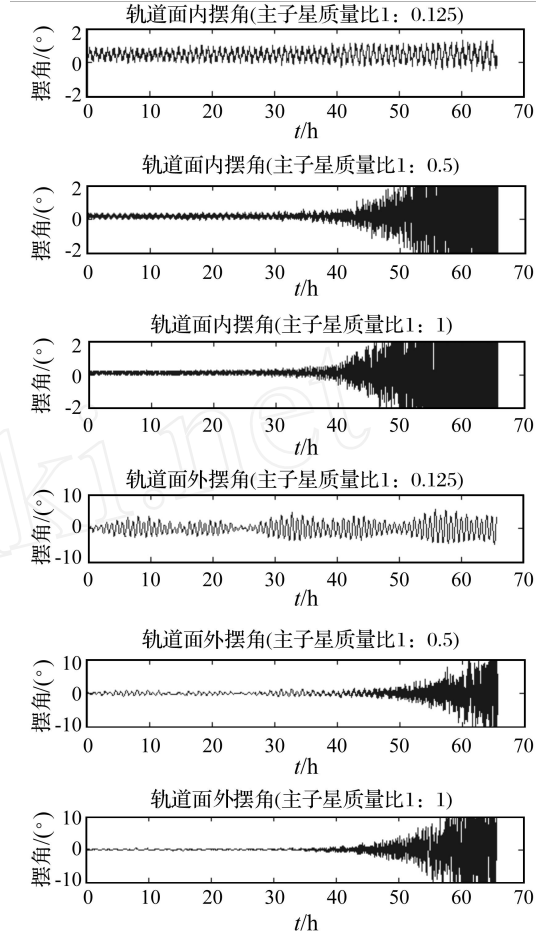

图 8 不同主子星质量比的导电系绳振荡摆角

2) 对于同一系统,系绳轨道面内摆角要比面外摆角小,面内摆动的频率也比面外的小。

3) 不同长度的导电系绳主要影响轨道面内振荡频率,对轨道面外而言仅影响其振动频率即高频振荡频率。

4) 主子星质量比越小,其导电系绳振荡频率成分越多,随着电动绳系系统推进时间的增加,系统偏离铅垂线角度逐渐增大,直至某一最大角度,此后保持该角度周期性地摆动。

参 考 文 献

[1] 许 滨,张 珩. 空间绳系技术及其应用[J]. 863航天航空技术, 2002, 10: 30—36.

[2] Samanta Roy R I, Hastings D E, Ahedo E. Systems Analysis of Electrodynamic Tethers[J]. Journal of Spacecraft and Rockets, 1992, 29(3): 415—424.

[3] Iess L, Bruno C, Ulivieri C, et al. Satellite De - orbiting by Means of Electrodynamic Tethers[J]. Acta Astronautica, 2002, 50(7): 399—406.

[4] Corsi J, Iess L. Stability and Control of Electrodynamic Tethers for De - orbiting Applications[J]. Acta Astronautica, 2001, 48(5 - 12): 491—501.

[5] Emmanuel Viennet, Alois Steindl, Hans Troger. Control of Electrodynamic Tether Vibrations in Space, Proc. Appl. Math. Mech., 2005, 5: 141—142.

[6] 肖业伦. 航天器飞行动力学原理[M]. 北京:宇航出版社, 1995.

© 1994-2009 China Academic Journal Electronic Publishing House. All rights reserved. http://www.cnki.net

studied. The switching matrix is given and the period-doubling bifurcation of periodic motions of the system is investigated by the Floquet theory. Poincaré map is established and further study on period-doubling bifurcations and chaotic behaviors in the non-smooth system is done by means of numerical simulations. The chaotic behaviors in the system are effectively controlled to the different periodic orbits using the coupling feedback control method and the constant load addition control method.

Key words: piecewise-linearity; Floquet theory; periodic motion; bifurcation; chaos; control (PP: 20 - 24)

ANALYSIS METHOD FOR TENSILE MEMBRANE STRUCTURES WITH SNOW LOAD

TIAN Jun, YE Ji-hong
(College of Civil Engineering, Southeast University Nanjing 210096, China)

Abstract: A method is given to redefine the basic snow pressure based on the expectation life of the membrane structures. Then the maximum entropy reliability theory is used to calculate the most possible deformation (displacement) of each node when the membrane structure bears full-span and half-span snow load. Finally, the surface stress distributions of the corresponding work conditions calculated by means of ANSYS are compared with those given by the current deterministic method. The result shows that the existing design method can be used to design the membrane with full-span snow. But for the half-span snow, the deterministic analysis method is unsafe for the light weight and load-sensitive membrane structure.

Key words: tensile membrane structures; snow load; the maximum entropy method; deterministic method (PP: 25 - 31, 98)

DESIGN AND REALIZATION OF ONLINE MODAL ANALYSIS SYSTEM FOR RUN YANG SUSPENSION BRIDGE

LI Zhi-jun, LIAi-qun, HAN Xiao-lin, MIAO Chang-qing
(College of Civil Engineering, Southeast University, Nanjing 210096, China)

Abstract: Run Yang suspension bridge is taken as the engineering background to study design and realization of the online modal analysis system, including design strategy, structure, sensor placement, location optimization and method of modal identification. Based on analysis for dynamics of the bridge, an optimal sensor placement system is put forward. Some important improvements on modal identification are made and used for realization of the online modal analysis. Most importantly, a method to identify modal parameters is put forward, which takes advantage of girder vibration mode functions to optimize modal parameters derived by peak picking method. Comparing the identification results from online modal analysis system with those from field measurement, the resulted modal frequencies and modal shapes are considerably consistent. Run Yang suspension bridge online modal analysis system is completed and operated over one year, which provides a large amount of parameters for analyzing the dynamics and evaluating the state of the bridge.

Key words: suspension bridge; online modal identification; evaluation; ambient excitation; modal test; modal shape optimization (PP: 32 - 35, 86)

DYNAMIC FEATURE ANALYSIS OF SPACE ELECTRODYNAMIC TETHER SYSTEMS

LI Ran, XU Bin, ZHANG Heng
(Division of Technology Development, Institute of Mechanics, The Chinese Academy of Sciences, Beijing 100080, China)

Abstract: With its mass and flexibility of an electrodynamic tether system considered, the propulsive motion of the electrodynamic tether system is modeled. Vibration and transmogrification features of the electrodynamic tether system are studied. The numerical solutions under various conditions are obtained, based on which the orbital motion of the electro-

© 1994-2009 China Academic Journal Electronic Publishing House. All rights reserved. http://www.cnki.net

dynamic tether system and the deformation of the tether are discussed.

Key words: electrodynamic tether system; tether; vibration; frequency (PP: 36 - 40)

NONLINEAR DYNAMICS STUDY ON A KIND OF GALLOPING PROBLEM

HE Xue-jun[1], *ZHANG Qi-chang*[1], *ZHANG Cui-ying*[1,2], *ZHANG Wen-de*[1]

(1. School of Mechanical Engineering, Tianjin University, Tianjin 300072, China;
2. Department of Civil Engineering, Hebei Engineering and Technical College, Cangzhou 061001, China)

Abstract: Nonlinear dynamics of a half cylinder model under aerodynamic load is studied. The model is analyzed by CFD software FLUENT and symbol algebra language Mathematica. The averaging method is used to analyze this model, the phase diagrams and the time history curve of this system are achieved, the results show that its movement converges to a limit circle oscillation. It demonstrates that the results obtained by the averaging method coincide with those by experiment well. A new method for study on galloping using CFD software Fluent and nonlinear dynamic theory is presented here.

Key words: nonlinear; galloping; averaging method; aerodynamic force (PP: 41 - 44)

EFFECT OF SHAPE FACTOR ON MECHANICAL CHARACTERISTICS OF METAL-RUBBER

LI Yu-yan[1], *HUANG Xie-qing*[2]

(1. Department of Mechanical and Electrical Engineering, Xi'an Technological University, Xi'an 710032, China;
2. Department of Mechanical Engineering, Xi'an Jiaotong University, Xi'an 710049, China)

Abstract: On basis of porous material theory, a model of force-displacement relation is constructed for a metal-rubber structure. Through fitting data of static experiments on the structure of a hollow cylindrical metal-rubber, the relations between coefficients of force-displacement model and shape factors are obtained. The relations between coefficients and the height or the loaded area of the structure are also obtained. Further, effect of shape factor on mechanical characteristics of metal-rubber is proved. Ultimately, prediction for the force-displacement relation of the metal-rubber structure is realized when the density is given and the shape factor are changed.

Key words: metal-rubber; porous materials theory; force-displacement relation; shape factor; height; loaded area (PP: 45 - 50, 54)

GEAR FAULT DETECTION BASED ON RELEVANCE VECTOR MACHINE

ZHOU Xiao-Ying, LI Wei-Hua, DING Kang

(South China Univ. of Tech. of Automotive Engineering, Guangzhou 510640, China)

Abstract: In order to solve a problem of insufficient samples in fault detection, a fault detection method based on relevance vector machine is presented. A separability evaluation function is constructed to direct the feature selection. A one-classification classifier is applied in gearbox fault detection, and the machine state can be recognized only using normal state samples. The experimental results show that relevance vector machine is superior to the support vector domain description method in terms of classification and computation.

Key words: relevance vector machine; one-classification; fault detection; feature selection (PP: 51 - 54)

THERMAL FLUTTER ANALYSIS OF A THREE-DIMENSION PANEL

YE Xian-hui, YANG Yi-ren

(Dept. of Appl. Mechanics and Eng., Southwest Jiaotong University, Chengdu 610031, China)

Abstract: Based on the first piston theory of supersonic aerodynamics, flutter differential equations of a three-dimension panel with thermal effect are set up according to Von Karman large deformation strain-displacement relation using

© 1994-2009 China Academic Journal Electronic Publishing House. All rights reserved. http://www.cnki.net